Misbehavior Forecasting for Focused Autonomous Driving Systems Testing

M M ABID NAZIRI*, North Carolina State University, USA
STEFANO CARLO LAMBERTENGHI†, fortiss GmbH, Germany
ANDREA STOCCO†‡, fortiss GmbH, Germany and Technical University of Munich, Germany
MARCELO D'AMORIM*, North Carolina State University, USA

Simulation-based testing is the standard practice for assessing the reliability of self-driving car software before deployment on public roads. Many automated testing techniques generate challenging simulation scenarios to maximize failure detection. However, these techniques require executing a large number of test cases to expose realistic failures. Yet, failure-free test cases may still contain segments where the autonomous driving system was close to a failure. These near misses are often overlooked, reducing testing effectiveness.

This paper focuses on enhancing the efficiency and effectiveness of automated testing for autonomous driving systems by focusing on near misses observed during simulation-based testing. Our approach, implemented in a tool called Foresee, identifies potential near misses using a misbehavior forecaster that computes possible future states of the ego-vehicle under test. Foresee performs local fuzzing in the neighborhood of each candidate near miss to surface previously unknown failures. In our empirical study, we evaluate the effectiveness of different configurations of Foresee using several scenarios provided in the CARLA simulator. Our results show that Foresee is both more effective and more efficient than the baselines. Foresee exposes 124.14% and 63.87% more failures than a random approach and a state-of-the-art failure predictor while being 2.62x and 1.44x faster, respectively.

Additional Key Words and Phrases: autonomous driving testing, misbehavior forecasting, focused testing

ACM Reference Format:
M M Abid Naziri, Stefano Carlo Lambertenghi, Andrea Stocco, and Marcelo D'Amorim. 2024. Misbehavior Forecasting for Focused Autonomous Driving Systems Testing. 1, 1 (August 2024), 21 pages. https://doi.org/10.1145/nnnnnnn.nnnnnnn

1 INTRODUCTION

Autonomous driving systems (ADS) are cyber-physical systems engineered to reduce human intervention in the operation of a vehicle. ADS have been attracting tremendous societal interest given their potential to mitigate transportation problems, including enhancing road safety and alleviating issues such as traffic congestion and commuting time [41]. Despite notable strides in autonomous driving software, concerns about ADS safety persist [8, 61]. For instance, in 2020, data

Authors' addresses: M M Abid Naziri, mnaziri@ncsu.edu, North Carolina State University, 2101 Hillsborough Street, Raleigh, North Carolina, USA, 27607; Stefano Carlo Lambertenghi, lambertenghi@fortiss.org, fortiss GmbH, Guerickestraße 25, Munich, Bayern, Germany, 80805; Andrea Stocco, stocco@fortiss.org, fortiss GmbH, Guerickestraße 25, Munich, Bayern, Germany, 80805, andrea.stocco@tum.de and Technical University of Munich, Boltzmannstraße 3, Garching near Munich, Bayern, Germany, 85748; Marcelo D'Amorim, mdamori@ncsu.edu, North Carolina State University, 2101 Hillsborough Street, Raleigh, North Carolina, USA, 27607.

XXXX-XXXX/2024/8-ART $15.00
https://doi.org/10.1145/nnnnnnn.nnnnnnn

from California's public roads revealed 43 collisions involving self-driving cars, leading to property damage, bodily injury, or fatalities [15].

Real-world physical testing of ADS, albeit important, has severe time, resource, and legal limitations [50]. For this reason, simulation-based testing [30, 35] has become the de-facto approach for ADS testing [53]. Simulators enable developers to assess the reliability of the ADS before deployment as they consist of virtual simulation platforms in which developers "plug" their ADS and test it against challenging conditions. A test describes a route that an ADS must complete within a map representing an urban environment containing static and dynamic objects (e.g., traffic signs and other vehicles). Researchers have used various open-source ADS simulators, including CARLA [16], LGSVL [45], BeamNG [3], and Udacity [58]. A plethora of commercial close-source solutions exist, such as Siemens PreScan [48], ESI Pro-SiVIC [20], and PTV VISSIM [62].

Prior work has been proposed to generate test cases for ADS, particularly leveraging search-based optimization [1, 4, 5, 19, 35, 36, 40, 44] and fuzzing [11, 26, 32, 34, 66], which are characterized by drawbacks in terms of effectiveness and efficiency. Concerning the former, these solutions require the exploration of a vast multi-dimensional search space to pinpoint critical conditions. This is problematic due to the significant time and resource overhead, as running a single test case on a driving simulation platform can take several minutes. About the latter, existing testing techniques either apply mutations *at the scenario level* in the initial state of a simulation, e.g., the number and position of the vehicles at the beginning of the simulation or guide the search relying on the *global* ADS behavior during the entire simulation or static features of test cases such as the number of bends of a road [6]. As a consequence, these techniques are oblivious to *near misses*, i.e., circumstances where a failure would occur with minimal modifications to certain intermediate states of a simulation in which the ADS was close to failure. Overlooking near misses limits the potential of test generators to reveal failures and potentially inflates the safety perception of ADS.

This paper aims to improve simulation-based testing of ADS in terms of effectiveness and efficiency by investigating the problem of *detecting and exploiting* near misses during virtual simulations. Instead of relying on global or initial states of a scenario-based test, we target focused testing of intermediate states occurring during failure-free simulations. We leverage the insight that critical scenarios may exist within driving simulations, where even minor modifications, such as slight speed adjustments at an intersection, could expose failures.

We propose FORESEE (FOREcasting unSafe Events and Emergency situations) a *focused* system testing technique for ADS. FORESEE uses a monitor to measure risk during the simulation of a given test case. It uses risk data to derive, classify, and prioritize short-running test cases. FORESEE fuzzes the inputs of these local and seemingly relevant test cases to find failures. More specifically, FORESEE uses telemetry data—obtained during simulation—to automatically identify conditions in which the system is close to a failure. This paper focuses on the identification of collisions, being the primary acceptance criteria for safe deployment of ADS. We show that telemetry data offers clues about the failure likelihood of the ADS. FORESEE uses telemetry data to forecast potential failing conditions, such as the identification of vehicles or pedestrians that are crossing the future trajectory of the vehicle under test. Hazardous driving conditions are detected when the failure likelihood increases in a future state of the simulation, as predicted by FORESEE.

We evaluated the effectiveness of FORESEE in the CARLA simulator [16], using ADS available from the literature and a diverse set of complex urban scenarios in which we observed many near-miss situations [55]. In our experiments on +1648 simulations accounting for more than 195 individual failures, FORESEE was able to surface up to 11.83% additional failures from near misses, a 63.87% increase with respect to SELFORACLE [52], a state-of-the-art misbehavior predictor based on autoencoders, and a 124.14% increase with respect to a random assessment of risk. FORESEE also demonstrates its efficiency against all the other baselines by discovering collisions 1.44x faster than

SelfOracle and 2.62x faster than Random. We also observed a 318.29% more efficient discovery of failures with the best-performing configuration of Foresee relative to a ground truth generated from an exhaustive search.

Our paper makes the following contributions:

Technique. A technique for ADS misbehavior forecasting based on ego vehicle kinetics. Our approach is implemented in the publicly available tool Foresee [57]. To the best of our knowledge, this is the first solution that uses vehicle kinetics to estimate the future states of a DNN-based ADS, surfacing potential failing situations from near misses. Foresee is complementary to existing, non-local, fuzzing techniques that ignore near misses.

Evaluation. An empirical study showing that Foresee outperforms a random and a black-box approach SelfOracle [52].

Dataset. A dataset of ADS failures in the CARLA simulator. The dataset can be used to evaluate the performance of failure prediction systems and test generators for ADS. The tool and evaluation data are publicly available [57].

2 BACKGROUND

2.1 Autonomous Driving Systems

ADS are software systems developed with increasing capabilities to drive vehicles autonomously. From an architectural point of view, ADS can be mainly divided into two categories: single-module ADS (a.k.a. end-to-end driving models) and multi-module ADS. The first category is based on advanced deep neural networks (DNNs) that are trained on massive driving datasets gathered by sensors, cameras, and GPS to perceive the environment. Once trained, models like NVIDIA's DAVE-2 [7] are capable of predicting the vehicle's controls (i.e., steer, brake, acceleration). The second category is comprised of ADS organized into four modules [2, 29, 64]: perception, prediction, planning, and control. The perception module receives as input various sources of sensory data, such as images of the front camera or proximity sensors to detect objects in the surroundings of the vehicle. The prediction module predicts the moving trajectories of these objects, which are used by the planning module to decide a safe route. The control module translates the planned route into vehicle driving commands, e.g., a sequence of steering angles.

End-to-end systems, in comparison to modular pipelines, benefit from joint feature optimization for perception and planning [10]. On the other hand, critical challenges exist regarding multi-modality, interpretability, and robustness, which motivated the development of multi-module ADS such as Pylot [43], Transfuser [12] or Interfuser [46]. As of now, the two approaches coexist [10, 64] and it is not clear if one approach will prevail over the other. In this paper, we consider testing multi-module ADS, while we left the investigation of end-to-end ADS for future work.

2.2 Simulation-based Testing of ADS

Driving simulation platforms are the de-facto choice in the industry for developing and testing ADS before real-world testing on roads [21, 22, 50]. High-fidelity simulators, such as CARLA [16] or LGSVL [45], replicate complex urban and highway driving scenarios using existing graphic assets representing buildings, pedestrians, and vehicles. These simulators generate a stream of simulated sensor data at regular intervals, such as data from cameras, that are fed to the ADS to enable motion within the simulated environment. The simulator relies on a model of physics that resembles real-world vehicle dynamics, allowing an accurate replication of vehicle behaviors and their corresponding trajectories. In the remainder of this section, we describe the nomenclature used in this paper.

Scenario. Scenarios are high-level characterization of vehicle movements and dynamics that are critical for testing. They often originate from transportation agencies, such as the US NHTSA (National Highway Traffic Safety Administration), which document such "pre-crash" circumstances from police reports. These scenarios provide a foundation for public and private organizations to test ADS and allow researchers to determine realistic safety issues to develop crash-avoidance systems [41]. A scenario describes the events that should happen throughout the simulation. These events include relevant actors, such as a pedestrian crossing a street outside of a crosswalk or a vehicle running a red light at an intersection, and the need for obstacle avoidance maneuvers involving pedestrians or other vehicles during driving. Scenarios differentiate static and dynamic objects. Static objects include traffic lights, crosswalks, and other urban infrastructure elements (e.g., trees). The placement of these objects is determined by maps, which define the topology of the streets. Dynamic objects include an ego vehicle, which is the vehicle controlled by an ADS–subject under test in this paper–and Non-Playable Characters (NPCs), which are objects within the simulation whose actions and behaviors are governed by predefined rules and behaviors.

Test Case. Given a scenario, a simulation-based test case is characterized by an *initial state* and a *route*. The initial state outlines the conditions of both static and dynamic objects at the beginning of the simulation, including the positions, velocities, and states of all objects in the scenario. The route specifies the path that the ego vehicle is expected to follow during the simulation. It is typically defined in terms of a starting and ending point or as a sequence of waypoints within the map that the ego vehicle should navigate through. To sum up, a route establishes a possible ground truth trajectory the ego vehicle should follow in the simulation. Together, these components establish the foundation of a simulation-based test case, allowing for the systematic evaluation of how the ego vehicle and other dynamic entities interact within a scenario.

Failures. ADS are designed to meet several requirements, encompassing factors about passenger safety and comfort [9]. Driving simulation platforms automatically log any rule violations that occur during testing. Among these, safety violations are of utmost concern, particularly when it comes to autonomous driving, as they can potentially lead to vehicle crashes and casualties.

This work focuses on predicting collisions. Collision avoidance is a primary prerequisite to be met as a self-driving vehicle must stay in its lane and prevent collisions to gain public trust and acceptance for production use. Our categories of failures include collisions involving the ego vehicle with elements beyond the road, such as pavements or poles, pedestrians, or other vehicles (Section 4.4).

3 APPROACH

Foresee aims to detect the occurrence of unexposed system failures during simulation-based testing of ADS. It builds on the observation that infractions are relatively rare compared to near misses. For example, on average, DriveFuzz [32] exposed 19 violations in 360 minutes (≈19 minutes per failure), whereas AV-Fuzzer [34] exposed on average 50 failures in 1000 simulations (20 simulations per failure) [66]. The unique aspect of Foresee is that *it exploits near misses observed during simulations* to detect failures.

A test suite *TS* consists of test cases associated with scenarios that are challenging for an autonomous vehicle (Section 2.2). For example, Scenario 4 of the CARLA leaderboard [55] deals with situations where the ego vehicle finds an obstacle on the road while performing a maneuver and it must perform an emergency brake or an avoidance maneuver.

Foresee focuses on failure-free test cases. More precisely, it focuses on finding *potentially missed failures in near-critical conditions*. It has to be noted that our technique could also be used to find further critical situations in failing test cases. We focus on failure-free scenarios because the high cost of simulation-based testing demands strategies that can reuse the simulation time required to

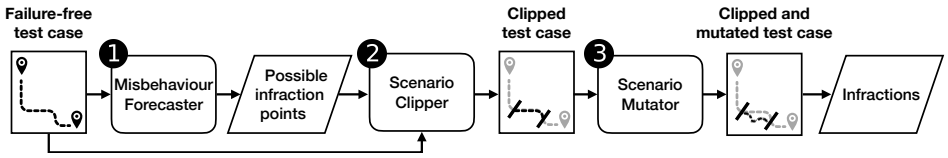

Fig. 1. An overview of Foresee.

produce near-critical circumstances and leverage them. It is also important to note that any failure-free simulation could, in principle, be turned into a failing simulation if aggressive or unrealistic mutations are applied, e.g., increasing the speed of the NPCs above the traffic limits by a large extent. It is critically important to retain the realism and intent of the original test scenarios. As such, Foresee makes small mutations to intermediate states of the simulation and applies several sanity checks to check if mutations are realistic.

3.1 Overview

Foresee takes as input a test case that does not reveal failures in nominal conditions (i.e., a failure-free test case) and reports infractions as output. Figure 1 illustrates the Foresee pipeline, consisting of three tasks, highlighted with numbers in the figure.

The Misbehavior Forecaster ❶ is responsible for identifying risky conditions during a simulation by tracking the position, speed, and steering angle of the NPCs at each time frame. Using the information in the collected execution traces, it then predicts what parts of the simulation are more likely to cause infractions. This component reports a ranked list of risky points sorted by a criticality score. Foresee attempts to find potential modifications in the original simulation around these risky points to reveal previously unforeseen failures. For that, it uses the Scenario Clipper ❷ to re-construct a feasible simulation in the neighborhood of a risky point. For each risky point, Foresee computes feasible start and end points from the original simulation that include the given likely infraction-inducing point. Then, it computes the NPCs that are relevant for that subset of the simulation. Finally, the Scenario Mutator ❸ introduces mutations in the initial states of the new simulations, effectively creating small variations on the intermediate states of the original simulation. At the end of the process, Foresee runs the derived (short) simulations and reports test cases revealing infractions.

To sum up, Foresee uses a combination of misbehavior forecasting, scenario clipping, and local scenario-level mutation to find unforeseen failures. It reports failure-revealing test cases without executing expensive fuzzing campaigns.

3.2 The Foresee pseudocode

Algorithm 1 shows the Foresee pseudocode. The algorithm takes as input a non-failing test case tc, the maximum number of risky points n_{rp} to detect in a run of tc, the number of child tests C to create per risky point found in tc's run, and the offsets o_a and o_b, defining the boundaries of the route for the tests derived from tc. Foresee reports a set of infractions O that the simulator observes with the execution of such derived (shorter) test cases.

Foresee runs a given test case tc and uses the Misbehavior Forecaster (Section 3.3) to retrieve a list of risky points RP (Line 1), revealing the parts of tc when risk was higher than a threshold. Each risky point in RP contains information about the simulation timestep[1] and the riskiness score the MisbehaviorForecaster reports. Intuitively, the higher the score the higher the risk.

[1]Simulation or game time is insensitive to the changes in resource availability during the execution of a simulation.

Algorithm 1: FORESEE.

Input : tc: a non-failing test case
n_{rp}: maximum number of risky points to detect in tc
C: number of children (i.e., tests derived from tc) per risky point
o_b: offset before a risky point
o_a: offset after a risky point
Output : O: A set of infractions

```
1 RP ← MisbehaviourForecaster(tc) (??)
2 relevant_RP ← first n_rp frames of RP
3 for rp in relevant_RP do
4     new = ClipScenario(tc.route, rp − o_b, rp + o_a) (Section 3.4)
5     for i in 1..C do
6         tc' = Mutate(GetRelevantNPCs(rp−o_b), tc.scenario, new) (Section 3.5)
7         O = O ∪ run(tc').failures
```

The risky points in *RP* are ranked by the riskiness score and a maximum of n_{rp} risky points are kept in *RP* while the rest are discarded. For each risky point rp (Lines 2-7), FORESEE proceeds as follows. The function CLIPSCENARIO (Line 4) determines the segment of the original route (field *tc.route*) that the ego vehicle should follow, i.e., it looks for the waypoints in the time period $[rp - o_b, rp + o_b]$ (Section 3.4). Each iteration of the inner loop (Lines 5-7) runs a test case tc' trying to expose new infractions. The function GETRELEVANTNPCS (Line 6) determines the NPCs that are near the ego vehicle (Section 3.5) and produces a state, which is passed as an input to the function MUTATE (Line 6). MUTATE defines a new state of a simulation by fuzzing the state from GETRELEVANTNPCS, e.g., it modifies the steering angle and the model of vehicles relevant to the ego vehicle (Section 3.5). Finally, FORESEE executes the newly constructed test case (Line 7) and adds observed failures to the output list. FORESEE uses the built-in oracles of the simulator to detect an infraction, e.g., collision with pedestrians (Section 2.2).

The following sections elaborate on each of the numbered steps of our approach.

3.3 Misbehavior Forecaster

Intuitively, any misbehavior predictor or anomaly detector from the literature can be used within FORESEE, such as those based on camera-frame image analysis with autoencoders [52] or clustering [11]. In this paper, we propose a novel type of predictor in which risk is assessed using telemetry data to forecast potential failing conditions, such as vehicles or pedestrians that are crossing the future trajectory of the vehicle under test.

The misbehavior forecaster takes a test case tc as input and returns a list of risky points ranked by their likelihood of causing an infraction. Figure 2 illustrates the four-step workflow of FORESEE to obtain the ranked list of NPCs, which we explain next.

Step 1: Proximity NPC identification. This step identifies the NPCs that approach the ego vehicle within a certain radius during the original simulation. For that, FORESEE computes the set *close_NPCs* describing the circumstance when NPCs are closest to the ego vehicle considering that radius. The set contains pairs with the simulation frame of the close encounter and the simulation ID of the corresponding NPC. Additionally, NPCs that are not within the radius are not considered (Discarded NPCs).

Step 2: Crossing NPC identification. For each NPC identified in the previous step, FORESEE retains those that cross the ego vehicle trajectory for further categorization. This filtering process yields two groups of NPCs: *Crossing_NPCs* contains NPCs that intersect with the ego vehicle path

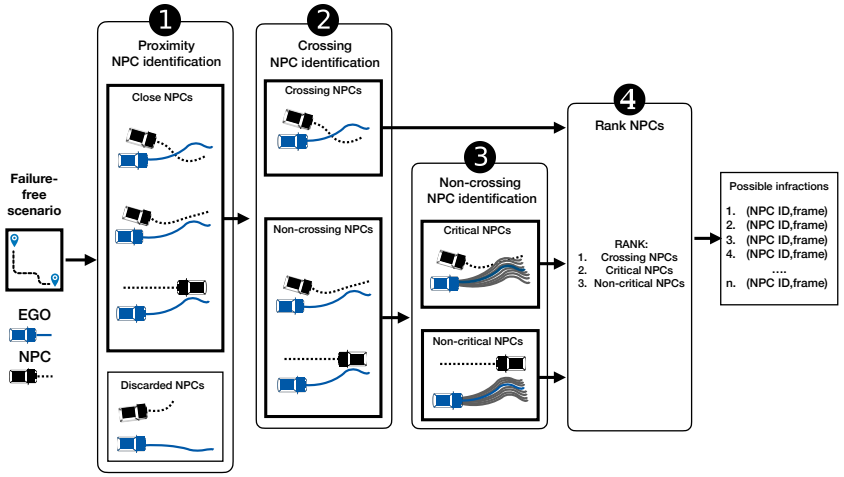

Fig. 2. Illustration of the logic of the Misbehavior Forecaster to produce a ranked list of NPCs that are likely involved in a risky condition with the ego vehicle under test.

during any simulation frame, and its subset, *Critical_crossing_NPCs*, includes NPCs that cross the ego vehicle but only within a limited distance from it.

Step 3: Non-crossing NPC identification. Algorithm 2 illustrates the logic that FORESEE uses to identify vehicle trajectories that could possibly result in collisions with the ego vehicle. The set $close\_non\_crossing\_NPCs = \{x \mid x \in close\_NPCs \text{ and } x \notin Crossing\_NPCs\}$ includes a list of NPCs that do not cross the path of the ego vehicle but come close to it. For each NPC in this set, the algorithm generates N perturbations of the original ego vehicle trajectory by introducing a small error in the velocity and yaw rate values. It then evaluates if any of the newly generated ego vehicle trajectories is below a distance *threshold* to the NPC. If so, FORESEE saves the NPC in the set *Critical_NPCs*. All *close_non_crossing_NPCs* ids that do not meet this distance requirement are saved in *Non-critical_NPCs*. The goal of this procedure is to account for the randomicity of the self-driving system under test, which could behave in a slightly different manner between different runs of the same scenario, therefore producing an unforeseen dangerous situation.

Step 4: Rank NPCs. In this step, FORESEE ranks the risky points associated with the NPCs in the aforementioned groups according to their risk (see Table 1) of causing a collision with the ego vehicle. If multiple NPCs are associated with the same risk level, FORESEE gives a higher score to NPCs that come closer to the ego vehicle trajectory during the simulation. For each of the ranked NPCs, our approach collects the simulation *frame* at which the actor comes closest to the ego vehicle during the nominal simulation.

3.4 Scenario Clipper

The scenario clipper component of FORESEE is responsible for creating a scenario reflecting solely the risky conditions observed during the execution of the original scenario. We use the term "clip" to indicate that only a subset of the original scenario is retained.

The top n_{rp} risky points of the list *RP* (Section 3.3) from $relevant_{RP}$ determine the timestamps to be clipped at, where n_{rp} is a hyperparameter that determines how many risky points should be considered for clipping. The parameters o_b and o_a indicate the length of the clip. For each risky point rp in $relevant_{RP}$, FORESEE clips the scenario from timestamp $rp - o_b$ to timestamp $rp + o_a$. To restore the state of the original simulation at timestamp $rp - o_b$, FORESEE saves the location,

Algorithm 2: Critical non-crossing NPCs detector.

Input : *close_non_crossing_NPCs*: list of actor ids
close_frames: matched list of frames
close_non_crossing_NPCs: a list of x, y and yaw
dt: time between two simulation frames
N: population size
T: time-range
$threshold$: distance threshold
MAX_{yaw}, MAX_v: minimum-maximum error ranges

Output: *Critical_NPCs* and *Non_critical_NPCs*: Two lists of actor ids

```
def computeYawRate() // yaw rate for each point in a trajectory
def computeVelocity() // velocity for each point in a trajectory
def computeNextPose() // given pose, yaw rate and velocity, returns the next pose
def computeDistance() // returns the closest point between two trajectories
for id in close_non_crossing_NPCs do
    t_start = close_frames[id] - T
    t_end = close_frames[id] + T
    ego_trajectory = trajectory_ego[t_start:t_end]
    yaws = computeYawRate(ego_trajectory)
    vels = computeVelocity(ego_trajectory)
    for id child in range(0, N) do
        ego_trajectories[id][child] = [trajectory_ego[0]]
        for frame in in range(1, range(1,t_end − t_start)) do
            (x, y, yaw) = new_ego_trajectories[id][child][−1]
            v_error = random(−MAX_v, MAX_v)
            yaw_error = random(−MAX_yaw, MAX_yaw) yaw = yaw + Yaws[frame] ∗ dt + yaw_error
            x = x + (Vels[frame] + v_error ∗ dt ∗ cos(yaw)
            y = y + (Vels[frame] + v_error ∗ dt ∗ sin(yaw)
            ego_trajectories[id][child].append(x, y, yaw)
            dist[id] = computeDistance(ego_trajectories[id][child], trajectory[id])
            min_dist[id] = min(dist[id], min_dist[id])
    if min_dist[id] < threshold then
        Critical_NPCs.append(id)
    else
        Non-critical_NPCs.append(id)
```

Table 1. Trajectory-based critical frames ranking.

Type	Data Origin	Risk Level
High risk crossing pedestrian	*Critical_crossing_NPCs* ∧ id=pedestrian	1
High risk crossing vehicle	*Critical_crossing_NPCs* ∧ id ≠ pedestrian	2
Medium risk crossing pedestrian	*Crossing_NPCs* ∧ id=pedestrian	3
Medium risk crossing vehicle	*Crossing_NPCs* ∧ id ≠ pedestrian	4
Medium risk non-crossing vehicle	*Critical_NPCs*	5
Low risk non-crossing vehicle	*Non_critical_NPCs*	6

direction, and model of each NPC. In this way, the clipped scenario is "centered around" the risky point rp. For timestamp $rp - o_b$, our approach stores the exact location of the ego vehicle at that timestamp. This information is useful to set the starting waypoint s_{wp} for the clipped scenario. Concerning the ending waypoint e_{wp}, the selection is more challenging. Indeed, we observed that

the location of the ego vehicle at timestamp $rp + o_a$ often results in invalid simulations in CARLA, because the simulator maintains specific sets of waypoints that can be used as a route in a scenario. As a working solution, our approach retrieves, from the log of the original simulation, a list of valid waypoints and uses the closest waypoint to the location of the ego vehicle at timestamp $rp + o_a$ as the ending waypoint e_{wp}. Finally, a new route XML file in which the clipped scenario starts at s_{wp} and ends at e_{wp}.

3.5 Scenario Mutator

For each clipped scenario, FORESEE applies several scenario-level focused mutations. The rationale is to assess whether the ego vehicle can cope with situations that are *analogous* to the one observed during the riskiest parts of the original simulation, yet they are slightly different and are expected to be more challenging. To maintain the validity and realism of the original simulation, the Scenario Mutator produces new short-lived simulations introducing modifications of the existing NPCs within the domain model and constraints of the CARLA simulator. This ensures that the resulting mutations are valid and realistic by design, as they operate within the NPC and kinematic space allowed in the CARLA simulator.

Specifically, our approach retains the original number of NPCs, while varying certain properties. First, the Scenario Mutator replaces the vehicle models for an NPC; for instance, a bicycle may be substituted with a car, which also affects the kinematic characteristics of the modified vehicle (i.e., the car is faster). The replacements are limited to the "relevant" NPCs in the neighborhood of the ego vehicle. To identify these relevant NPCs, the misbehavior forecaster reports a ranked list of NPCs that approached the ego vehicle along with the time frame in which they were closest (GETRELEVANTNPCS, Line 6 of Algorithm 1). FORESEE uses this information to select the NPCs for which their time frame lies within the interval $[rp - o_b, rp + o_a]$, where rp denotes riskiest point selected from the ranked list (Line 2 of Algorithm 1) and o_b and o_a denote, respectively, the offsets before and after the risky point delimiting the period of a new simulation.

The Scenario Mutator also ensures that the newly mutated vehicle model avoids collisions with other NPC vehicles upon spawning at the beginning of the simulation, potentially due to the increased length of the new model. To achieve this, our approach computes the distances between each pair of NPC vehicles and retains only the valid vehicle models. A valid vehicle model fits within the gap between two adjacent NPCs and does not cause immediate collisions. Additionally, certain sensors on the map at the initial point of a simulation can be placed as invisible objects, causing collisions with NPC vehicles if placed directly on the road. To avoid inflating the number of collisions with these phantom objects, we increment the z-axis value of the locations by a small constant value, denoted as z_offset, when saving the location. Since the simulator accounts for gravity, these vehicles are automatically positioned on the ground upon spawning.

Secondly, FORESEE adjusts the initial steering angle of the closest NPC to the ego vehicle as another form of mutation. To introduce variations in the steering angle, FORESEE tracks the closest vehicle to the ego vehicle $npc_{closest}$ in a test case at the beginning of the risky interval, i.e., at $rp - o_b$. Afterwards, for each child simulation, the Scenario Mutator applies a random steering angle to $npc_{closest}$. The simulator accepts scalar values within the range of $[-1.0, 1.0]$, a value within this range is randomly selected for the steering angle. Subsequently, FORESEE proceeds to generate C mutated children (Section 3.4), executing them, and reporting the number of collisions.

3.6 Example

Figure 3 shows an illustrative example of FORESEE. The images **A** and **B** display consecutive snapshots of a nominal failure-free simulation. Note that the (future) trajectory of the ego vehicle and the trajectory of the NPC vehicle would eventually cross. However, due to the low speed of the

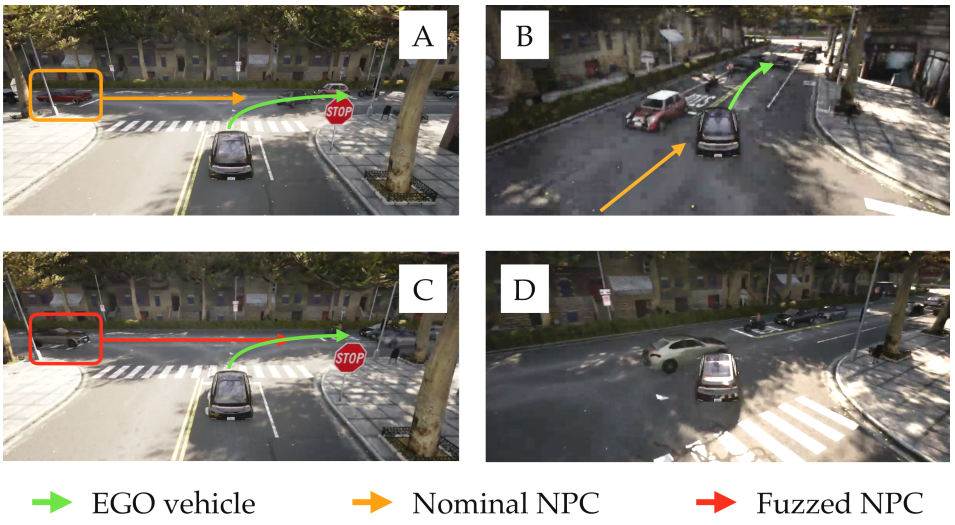

Fig. 3. Illustrative example showing a near miss from a failure-free simulation (top frames) and collision from a mutated simulation (bottom frames).

NPC, the two vehicles do *not* collide (image **B**). We refer to such missed cases from the original simulations as "near misses".

Images **C** and **D** display a failure condition that FORESEE reports. FORESEE identifies the segment of the simulation at which the vehicles would have eventually intersected as a risky point. Then, it "clips" the risky segment from the original simulation and creates new focused simulations derived from the clipped segment. In this example, the new simulation is obtained by mutating the model of the NPC vehicle (image **C**). The new simulation results in a collision between the ego vehicle and the mutated NPC, which is faster than the NPC from the original simulation (image **D**).

4 EVALUATION

4.1 Research Questions

We consider the following research questions.

RQ$_1$ (Effectiveness): *How effective is FORESEE in exposing misbehaviors in near-miss scenarios relative to an exhaustive search? How does effectiveness vary with different clip sizes and number of child tests?*

RQ$_2$ (Comparison): *How does FORESEE compare with alternative misbehavior prediction techniques (RANDOM and SELFORACLE)?*

RQ$_3$ (Efficiency): *How efficient is FORESEE in exposing misbehaviors in near-critical situations?*

The first research question evaluates the ability of FORESEE to detect near misses and generate failures. We evaluate effectiveness when varying two important parameters: the size of the clipped scenarios (as per o_a+o_b) and the number of near misses to exploit in each test (as per n_{rp}). Intuitively, longer clips and a higher number of risky points may reduce the tool's efficacy as the technique is tailored for targeted risk selection. We also compare the precision of FORESEE against an impractical EXHAUSTIVE approach that approximates an upper bound on the possible number of failures by applying fuzzing at each timestamp (excluding the first o_b seconds).

Table 2. Characterization of scenarios of Town10.

Id	Description	# tests
3	Obstacle avoidance without prior action	16
4	Obstacle avoidance with prior action	46
7	Crossing traffic running a red light at an intersection	19
8	Unprotected left turn at an intersection with oncoming traffic	19
9	Right turn at an intersection with crossing traffic	20

The goal of the second research question is to measure the ability of FORESEE's misbehavior forecaster component (Section 3.3) to detect risky points. We compare FORESEE against two baseline approaches, namely RANDOM and SELFORACLE. The RANDOM baseline selects a waypoint for local fuzzing at random, clips the simulation around that waypoint, and mutates its corresponding initial state. The second approach replaces the kinetics-driven misbehavior forecaster of FORESEE with SELFORACLE [52], a data-driven misbehavior predictor for ADS based on autoencoders.

The third research question evaluates how fast FORESEE exposes misbehaviors. We hypothesize that FORESEE exposes failures faster because only parts of the original simulation are used and executed. This research question evaluates this hypothesis.

4.2 Objects: Simulator, Scenarios, and ADS

4.2.1 Simulator. We used the CARLA simulator for self-driving cars [16] (v. 0.9.10.1), a driving simulator developed with the Unreal Engine 4 [17] used in previous ADS testing literature [32, 36, 66]. We chose CARLA as it supports complex urban scenarios with many configurations of static and dynamic objects, and provides a rich set of sensors (e.g., cameras, LiDAR, GPS, and radar) to enable the observation of the status of the ADS throughout the simulation.

4.2.2 Scenarios. CARLA supports various closed-loop urban maps for testing ADS. This paper considers Town10, one of the default maps provided by CARLA, with its default environmental configuration (e.g., sunny weather). Each map is covered by driving scenarios and each scenario is covered by different test cases. Within Town10, we consider five scenarios (see Section 2.2). Scenario 3 involves instances where non-player characters (NPCs) like pedestrians cross the road in front of the ego vehicle, which must execute avoidance maneuvers, such as emergency braking. Scenario 4 involves obstacles, such as crossing pedestrians, appearing on the road immediately after the ego vehicle has executed a maneuver, like a left turn. The ego vehicle must then take action to avoid collisions. Scenario 7 deals with situations where NPCs disregard traffic signals, specifically running a red light. The ego vehicle must maneuver to avoid potential collisions. Scenario 8 includes the ego vehicle executing a left turn at an intersection, yielding to oncoming traffic. Scenario 9 involves the ego vehicle making a right turn at an intersection while yielding to crossing traffic. Table 2 summarizes the scenarios and test cases for Town10.

4.2.3 ADS under Test. We use INTERFUSER [46], a reference model which sustains one of the highest scores in the CARLA leaderboard [54] and was used as the state-of-the-art in prior work [25, 27, 28]. INTERFUSER is an ADS model based on a multi-modal fusion transformer designed to operate in challenging scenarios with dense traffic. INTERFUSER uses images from three camera sensors (front-facing, left, and right) and LiDAR sensor data as input and generates driving commands such as steering, throttle, and brake. In addition, they use interpretable intermediate features (e.g. ego vehicle's trajectory, traffic signals) to keep the driving commands under a certain safety threshold. Architecturally, it uses ResNet34 and ResNet18 [23] to extract features from the input data and uses

transformers [60] to fuse them. This representation is processed by a single-layer Gated Recurrent Unit (GRU) [13] to predict the ego vehicle trajectory. Passing this representation through multi-layer and single-layer perceptrons respectively reveals the object density map and state of the traffic signal. Finally, the safety controller takes the trajectory, object-density map and the traffic signal states to determine low-level driving commands within a safe set.

4.3 Comparison Baselines

We compare FORESEE with three variations of our approach. These baselines use the previously defined Scenario Clipper (Section 3.4) and Scenario Mutator (Section 3.5), but replace the misbehavior forecaster with different alternatives, described below.

EXHAUSTIVE. The EXHAUSTIVE comparison baseline approximates an upper bound on the number of failures that our approach can observe if enough time and resources were available to explore the search space exhaustively. It is worth noting that EXHAUSTIVE is very expensive and impractical in real-world scenarios. The EXHAUSTIVE approach considers each second of the original simulation as the center of a clip regardless of its risk score, and constructs mutated sub-simulations from these clipped scenario segments. For example, with $o_b = o_a = 3$ (i.e., a 6s clip), a 48s simulation would be split into 45 points (first o_b seconds of the simulation omitted to ensure the validity of the constructed simulations), generating 45 clips of 6s each. It is worth noting that these simulations may have plenty of overlapping regions, contributing to an impractically large overhead in resource consumption. However, mutations can modify these overlapping states differently depending on the starting time of the clip. A comparison with this baseline demonstrates how far a technique is from revealing all possible failures, i.e., the EXHAUSTIVE baseline constitutes an approximation of the ground truth in terms of near misses.

RANDOM. This approach randomly selects waypoints from the original route and uses them as focal points for clipping and fuzzing. For this baseline, instead of using a score from the misbehavior forecaster to determine which waypoints in the original route are risky, we randomly select waypoints from the original route and apply clipping and mutation around them. A comparison with this baseline aims to show how FORESEE compares against a technique that does not use any guidance to select segments for local fuzzing.

SELFORACLE. SELFORACLE [52] is a black-box ADS misbehavior predictor [52]. Even if SELFORACLE was not proposed for test generation, this baseline is relevant because SELFORACLE is designed to detect risky situations that result in failures of ADS. Thus, in this paper, we use it as a baseline to detect near misses for local fuzzing.

Although SELFORACLE was originally developed, integrated, and experimented on the Udacity simulator [58], the approach is simulator agnostic. SELFORACLE requires images captured by the front-facing camera for training and inference. We use the best configuration of SELFORACLE presented in the original paper, i.e., a variational autoencoder (VAE) that reconstructs driving images and uses the reconstruction loss as a measure of confidence. The VAE has a latent size of two and it is trained to minimize the mean squared error (MSE) between the original and reconstructed images. For training SELFORACLE, we collected 151 images at 20 FPS from the map of "Town10" since this map is used in all of our experiments.[2] The autoencoder uses the Adam optimizer [33] to minimize the mean squared error (MSE) loss over 10 epochs, using a learning rate of 0.001. During inference, each frame of the simulation produces a front-camera image captured by the RGB camera sensor placed at the front of the ego vehicle. SELFORACLE takes these images as input and computes

[2]We could not obtain the original training set from the INTERFUSER [46] paper; thus we collected several images that are in line with what described in the paper, i.e., 125k for "Town10" at 2 FPS. We reduced the cardinality of the training set for SELFORACLE to avoid overfitting the autoencoder. Indeed, if an excessive number of images are provided, the autoencoder generalizes to risky situations, losing its predictive power, which is also acknowledged in the literature [51].

Table 3. RQ_1: Effectiveness of FORESEE. Breakdown of collisions per scenario and configuration. #RP=Number of risky points. #Colls. = Number of collisions.

clip dur.=6s	# risky points						
	1		2		4		EXHAUSTIVE
	#RPs	#Colls.	#RPs	#Colls.	#RPs	#Colls.	#Colls.
Scenario3	15	2.67	30	6	59	13.33	51
Scenario4	36	3	68.33	13	97.33	31.33	128.33
Scenario7	12	7.33	26	14	40	16.33	66.33
Scenario8	14	0	30	4.67	44	7	18
Scenario9	14	3.33	25	3.33	35	5	7.33
Σ	91	16.33	179.33	41	275.33	73	271

clip dur.=10s	# risky points						
	1		2		4		EXHAUSTIVE
	#RPs	#Colls.	#RPs	#Colls.	#RPs	#Colls.	#Colls.
Scenario3	15	5.67	30	8.33	59	13.33	34.67
Scenario4	35	11.33	66	26	95	39	77.67
Scenario7	11	0.67	25	6.67	41	21.67	68
Scenario8	13	2.33	28	12	42	14.33	46.33
Scenario9	14	4	25	4	37	5.33	6.67
Σ	88	24	174	57	274	93.67	233.33

a reconstruction error for each frame. Since each route used by the simulation is a set of waypoints, we divide each route into segments, each consisting of a pair of waypoints. For each segment, we compute the average of the reconstruction errors within that segment. This average value indicates the risk of the segment and we rank simulation segments by this risk value. We set a threshold $\gamma = 0.95$ for the expected false alarm rate in nominal conditions to identify risky conditions. A comparison with this baseline helps to demonstrate the effectiveness of FORESEE's misbehavior forecaster relative to a state-of-the-art anomaly detector.

4.4 Experimental Setup

To answer **RQ_1**, we execute various configurations on the scenarios from Table 2 and their corresponding test cases. We also compare the results of FORESEE against EXHAUSTIVE (Section 4.3). To identify NPCs in the proximity of the ego vehicle, we used the thresholds $th_1 = 10m$ and $th_2 = 50m$ for vehicles and pedestrians, respectively. For non-crossing NPC identification, we use the $threshold = 2m$. These values were tuned during preliminary pilot experiments which are not reported for the sake of space. For each near miss, we clipped the test case in a way that the near miss is contained within the offsets o_b and o_a. For simplicity, we considered $o_b = o_a$. For each clipped test case, we generate $C = 4$ mutated test cases by injecting mutations according to Section 3.5 and execute the clipped and mutated test cases. We determine the number of risky points to analyze as follows. For each simulation, we identify risky points and consider the top n_{rp} risky points from the ranked list that the misbehavior forecaster (Section 3.3) reports, unless the number of risky points identified is less than n_{rp}, in which case we consider all identified risky points. We obtain the number of risky points n_{rp} from the set $\{1, 2, 4\}$. Considering the length of the generated test cases, we consider $o_b = o_a \in \{3, 5\}$, thus enabling sub-simulations 6s and 10s long. For EXHAUSTIVE, we extract all possible 6s and 10s clips from the original test cases by treating each second of the simulations as risky points, i.e. taking $o_a + o_b$ seconds long cuts around each second of the original simulation. We use the number of collisions as the key performance metric for this research question (Section 2.2). We apply mutation operators on these clips and run the experiments with the same mutation count (C), compute and report the number of collisions for comparison. Overall, our experiment evaluates 6 configurations of FORESEE (i.e., 3 risky points $\times$ 2 simulation lengths). We empirically observed that shorter times are likely to produce invalid simulations whereas longer times jeopardize the benefits of local fuzzing and simulation reuse.

To answer **RQ_2**, we execute RANDOM and SELFORACLE with the same experimental setup from RQ1. More precisely, we use the same set of scenarios and tests (Table 2), the same set of mutation operators (Section 3.5), and the same configurations of FORESEE (i.e., combinations of clip size and offsets).

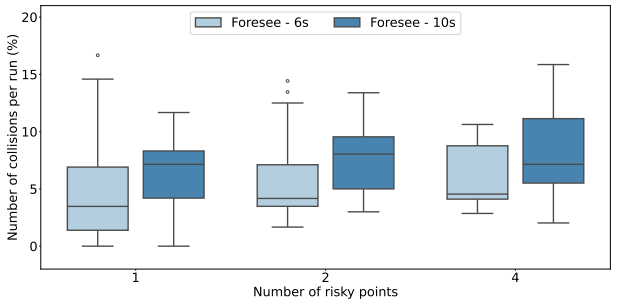

Fig. 4. RQ$_1$: Effectiveness of FORESEE on different configurations, i.e., choice of clip duration ($o_b + o_a \in \{6, 10\}$) and number of risky points ($n_{rp} \in \{1, 2, 4\}$).

To answer **RQ$_3$**, we log the time that each failure was observed and report the failure rate over time as an area under the curve (AUC). In this case, the x-axis of the curve indicates time and the y-axis of the curve indicates the cumulative number of failures observed. Intuitively, the larger the area the better the efficiency.

To cope with the non-determinism of the driving platform, we executed all the experiments 3 times and reported averages. Our dataset has a total of 120 routes from 5 scenarios, 17 of which have infractions when executed. Consequently, we discarded those cases, leaving 103 routes (i.e., test cases). Each of these test cases is considered seed scenario and from each of these test cases, we derive a maximum of 4 risky points. We construct clipped and mutated scenarios from this collection of risky points, which yields a total of 1648 test cases across 6 configurations ($n_{rp} \in \{1, 2, 4\} \times (o_b + o_a) \in \{6s, 10s\}$) and 3 repetitions. Overall, considering all configurations, we executed a total of 19776 test cases (3 techniques $\times$ 4 mutations $\times$ 1648 routes). It is worth noting that although test cases derived from the original input test are designed to be short running (i.e., 6s and 10s long), in practice they tend to take longer than the estimated time because of traffic signals and vehicles getting stuck during the simulation. In our setting, our simulations took on average 15s for 6s-clips and 30s for 10s-clips. Thus, the average simulation time is 22.5 seconds, with the estimated total computing time of our experiments being more than 123.6 hours ($22.5 * 19776/3600$) or more than five days. For the EXHAUSTIVE search, we created clipped and mutated sub-simulations from each second of each seed scenario (we omit the first o_b seconds for each seed scenario as it is not possible to obtain a valid simulation otherwise). In total, this process took around 43 days across 3 repetitions.

4.5 Results

4.5.1 RQ$_1$. Figure 4 shows distributions of *failure rates*, defined as the number of collisions detected per risky point, that FORESEE observes for different combinations of clip duration ($o_b + o_a \in \{6, 10\}$) and number of risky points ($n_{rp} \in \{1, 2, 4\}$). A data point in a distribution consists of the percentage of failures revealed by test runs of a given scenario (Table 2). Consequently, each distribution has 15 data points (5 scenarios $\times$ 3 repetitions). Note that each data point aggregates, as a percentage, results from several test runs. The figure reports three groups of boxplots with each group representing a different number of risky points (1, 2, or 4). In each group, we further differentiate between different clip durations (6s or 10s).

Table 3 details the results. The table reports, for different clip durations (6s or 10s), the number of risky points (#RP) and collisions (#Colls.) for different numbers of risky points (1, 2, or 4). For comparison, the column "#Colls." under EXHAUSTIVE represents the maximum number of collisions detected in an exhaustive search (Section 4.3). Intuitively, as the number of risky points increases, FORESEE exposes more failures over time. For clip duration=6s, the failure rate is 17.95% (16.33/91)

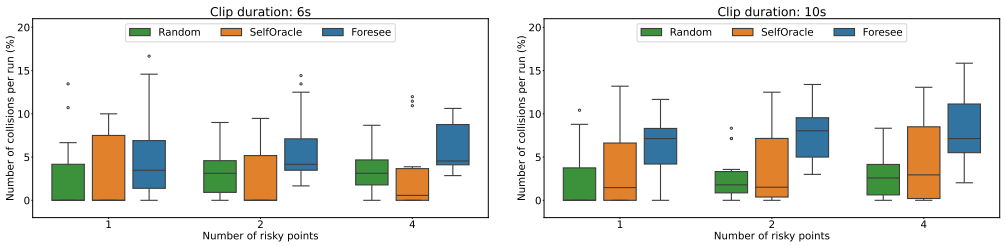

Fig. 5. RQ_2: Comparison of techniques over different configurations.

when one risky point is selected, 22.86% (41/179.33) when two risky points are selected, and 26.51% (73/275.33) when four risky points are selected. Similar considerations hold for the clip duration=10s where we observe failure rates of 27.27% (24/88), 32.76% (57/174), 34.19% (93.67/274) for the configurations with 1, 2, and 4 risky points selected, respectively. The Exhaustive column demonstrates the number of collisions discovered by the exhaustive search and acts as the ground truth for the potential collisions discoverable by Foresee. For $o_b + o_a = 6$ and $n_{rp} = 4$, Foresee discovers 73 collisions compared to 271 collisions discovered by Exhaustive, demonstrating 26.94% coverage by Foresee at this configuration. Similarly, for $o_b + o_a = 10$ and $n_{rp} = 4$, coverage for Foresee is 40.14% (93.67x 100 / 233.33), demonstrating the best coverage amongst the 6 configurations of Foresee.

RQ_1: How effective is Foresee in exposing misbehaviors in near-miss scenarios relative to an exhaustive search? How does effectiveness vary with different clip sizes and number of child tests?

Foresee exposes many collisions in near misses situations, with failure rates ranging over the interval 17.95-34.19% (26.94-40.14% near-misses coverage). We find the configuration with clip duration=10s and a number of risky points=4 to provide the best trade-off, quantified by failure rate.

4.5.2 RQ_2. Figure 5 shows the distributions of number of collisions for Foresee, SelfOracle, and Random. The left figure shows the results for clip duration=6s whereas the right figure shows the results for clip duration=10s. Overall, Foresee outperforms the baselines over all configurations. We measured the statistical significance of the differences using the non-parametric Mann-Whitney U test [63], with $\alpha = 0.05$, and the magnitude of the differences using the Cohen's d effect size [14]. For most configurations, the differences between Foresee and both baselines are statistically significant (6x2, 6x4, 10x2, and 10x4), i.e., the p-value < 0.05 with a medium/large effect size. For some configurations (6x1 and 10x1), only the differences between Foresee and Random are statistically significant, with medium/large effect sizes.

We provide detailed comparisons for the configuration 10x4, which is the one with the best failure rate from RQ_1. Table 4 shows the total number of failures for each technique. Column #TCs shows the number of test cases associated with a given scenario. Columns F1, F2, and F3 show the different kinds of collisions detected, respectively related to collisions involving the ego vehicle with elements beyond the road, such as pavements or poles (F1), pedestrians (F2), or other vehicles (F3). Column Σ shows totals. Results are presented for each scenario separately, as well as an aggregate. The table reinforces the effectiveness of Foresee over the baselines, across all scenarios and failure types. Overall, Foresee achieves a failure rate increase of +124.14% and +63.87% with respect to Random and SelfOracle, respectively. It also achieves a higher diversity of failure kinds observed, even though failure F3 (collisions with other vehicles) is the most prevalent.

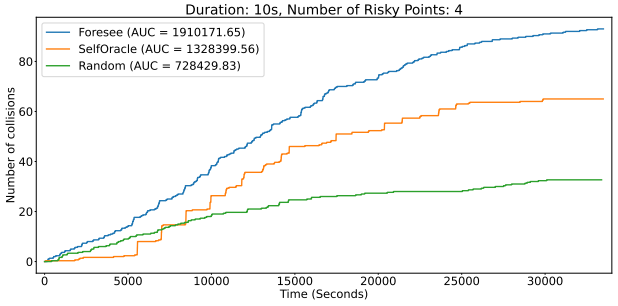

Fig. 6. RQ$_3$: Efficiency of the techniques.

RQ$_2$: How does FORESEE compare with alternative misbehavior prediction techniques (RANDOM and SELFORACLE)?

FORESEE outperforms the considered baselines, with a failure rate increase of +124.14% and +63.87% with respect to RANDOM and SELFORACLE, respectively.

4.5.3 RQ$_3$. The EXHAUSTIVE search showed the maximum number of collisions discoverable, but FORESEE is more efficient in finding the collisions. For $o_b + o_a = 6s$ and $n_{rp} = 4$, EXHAUSTIVE exposed 4.2 collisions per hour (271/64H) compared to 15.53 collisions per hour (73/4.7H) by FORESEE, resulting in a 269.76% efficiency increase. Similarly, for $o_b + o_a = 10s$ and $n_{rp} = 4$, EXHAUSTIVE discovered 3.5 collisions per hour (233.33/66.5H) compared to 14.64 collisions per hour (93.67/6.4H) discovered by FORESEE, a 318.29% increase.

Figure 6 shows the cumulative number of collisions detected by the techniques over time and the area under the curve (AUC) associated with the corresponding plots. The result indicates the superior ability of FORESEE over the baselines to efficiently expose failures, as evidenced by the position of FORESEE's plot relative to the plot of the other techniques (and higher AUC score). FORESEE has an AUC score of 1910171.65, which is 1.44x (1910171.65/1328399.56) higher than the AUC score of SELFORACLE and 2.62x (1910171.65/728429.83) higher than the AUC score of RANDOM. To sum up, results confirm that FORESEE detects more collisions than the baselines (as RQ2 has shown) and that FORESEE detects them faster.

RQ$_3$: How efficient is FORESEE in exposing misbehaviors in near-critical situations?

Results indicate that FORESEE detects collisions much faster compared to the baselines. The AUC of FORESEE is 1.44x higher than SELFORACLE's and 2.62x higher than RANDOM's.

Table 4. RQ$_2$: Comparison of RANDOM, SELFORACLE, and FORESEE. Configuration 10 x 4 ($o_b + o_a = 10, n_{rp} = 4$).

		RANDOM				SELFORACLE				FORESEE			
	#TCs	F1	F2	F3	Σ	F1	F2	F3	Σ	F1	F2	F3	Σ
Scenario3	235	0	5	2.67	7.67	0	2	1.67	3.67	0	9.33	4	13.33
Scenario4	390	0.67	0	13.67	14.33	0	0	40	40	0.67	0	38.33	39
Scenario7	167	0	0	4.67	4.67	0	0	18.67	18.67	0	0	21.67	21.67
Scenario8	179	0.33	0	5.33	5.67	0	0	2.33	2.33	0	0	14.33	14.33
Scenario9	145	0	0	0.33	0.33	0	0	0.33	0.33	0	0	5.33	5.33
Σ	1116	1	5	26.67	32.67	0	2	63	65	0.67	9.33	83.66	93.66

4.6 Threats to Validity

Internal Validity. All variants of FORESEE, SELFORACLE, and random were compared under identical experimental settings and on the same evaluation set. Thus, the main threat to internal validity concerns our implementation of the test scripts to evaluate the scores, which we tested thoroughly. Moreover, we could not train SELFORACLE with the same training set as INTERFUSER and we could not use any pre-trained model as they were developed for another simulator. We mitigated this threat by training the VAE following the existing guidelines [51, 52]. Indeed, our version of SELFORACLE shows competitive results concerning RANDOM and FORESEE. Concerning the ADS model, which could inflate the results if inappropriate for the task of driving, we used a publicly available ADS which achieved remarkable results in the CARLA leaderboard. Regarding the simulation platform, we used the CARLA simulator adopted in analogous failure prediction studies [59]. However, it is important to note our approach is independent of the chosen simulation platform. Other open-source propositions are available, such as Udacity [58] and BeamNG [3] but they mostly deal with lane-keeping ADAS [19, 44] and have no NPCs. We did not consider commercial close-source solutions such as Siemens PreScan [48], ESI Pro-SiVIC [20], and PTV VISSIM [62] as they do not allow full replicability of our results.

External Validity. The limited number of self-driving systems in our evaluation constitutes a threat to the generalizability of our results to other ADS. Moreover, results may not generalize, or generalize differently, when considering other simulation platforms.

5 RELATED WORK

5.1 Test Generation for Autonomous Driving

The majority of test generation techniques employ search-based techniques to automate the construction of test cases for DNN-based ADS [1, 4, 5, 31, 39, 42, 44, 56, 65]. In this domain, test cases can be either individual driving scenes images, or road topologies that are rendered using a 3D driving simulator. Abdessalem et al. [1, 4, 5] combine genetic algorithms and machine learning to test a pedestrian detection system. Mullins et al. [40] use Gaussian processes to drive the search-based test generation towards yet unexplored regions of the input space, whereas Gambi et al. [19] propose search-based test generation for ADS based on procedural content generation. Fahmy et al. [18] apply clustering to LRP heatmaps capturing the relevance of the DNN predictions to automatically support the identification of failure-inducing inputs. Zohdinasab et al. [67] use illumination search to cover a feature map of external behaviors of an ADS. Lu et al. [36] use reinforcement learning to learn environment configurations that lead an ADS to crash.

DriveFuzz uses the physical states of the vehicle and oracles based on real-world traffic rules to guide the fuzzer towards finding misbehaviors [32]. AutoFuzz [66] focuses on fuzzing the test scenario specification. Before fuzzing, it uses a seed selection mechanism based on a binary classifier that selects likely traffic-violating seeds. AV-Fuzzer [34] uses a genetic algorithm that is informed by the positioning of globally monitored NPCs in each scenario in the driving environment. The NPCs with higher potential of safety potential [26] violation likelihood are selected for evolution. Cheng et al. [11] propose BehaviorMiner, an unsupervised model that extracts the temporal features from certain given scenarios and performs a clustering-based abstraction to group behaviors with similar features into abstract states.

Test generators are designed to maximize the number of failures and consider whole test cases. While the exploration is guided towards critical regions, the search budget is consumed by running test cases that do not result in failing conditions. Our approach differentiates itself by forecasting potential ego vehicle states to predict infractions with NPCs and focuses on local segments within test cases. Existing fuzzers/test generators do not constitute direct baselines for our approach, as

they operate at the beginning of each scenario by creating new test scenarios at each iteration to maximize failure exposure. Thus, no simulation effort is reused as they operate globally, other than locally. However, they can be used in conjunction with FORESEE to improve their effectiveness, especially for the false negative cases. We leave this exploration for future work.

5.2 Anomaly Detection in Autonomous Driving

We already discussed SelfOracle [52], for which we performed an explicit empirical comparison in this work. Similarly, DeepGuard [24] uses the reconstruction error by VAEs to prevent collisions of vehicles with the roadside. ThirdEye [49] uses the attention maps from the explainable AI domain to predict misbehaviors of self-driving cars, whereas other researchers [37, 38] use Bayesian inference methods for probabilistic safety estimation. DeepRoad [65] validates single driving images based on the distance to the training set, using embeddings rooted in the features extracted by VGGNet [47].

Our approach differs from the aforementioned approaches because it uses a risky score of the system synthesized from a forecasting mechanism of the ego vehicle kinetics.

6 CONCLUSIONS

Simulation-based testing is highly useful in autonomous vehicle testing, but the cost of revealing faults relative to the time to run simulations is very high. We propose FORESEE, an approach to optimize simulation-based testing by reusing segments of simulations that produce near-failing situations. Our approach uses a custom misbehavior forecaster to detect near misses and fuzz the state of the simulation locally (i.e., close to the critical regions) to produce failures quickly. Our experiments revealed that (1) failure-free scenarios embed many near-failing situations that FORESEE can accurately detect and that (2) many of these cases result in failures when minimal perturbations are introduced. FORESEE provides initial yet strong evidence that guiding fuzzing with misbehavior forecasting is a promising approach to uncovering hidden failures in ADS.

In the future, we plan to conduct a qualitative analysis of the near misses found in this study and to evaluate whether they are useful in improving the robustness of the ADS. We also plan to evaluate additional infraction scenarios, towns, and autopilots to deepen the evaluation of the hyper-parameters of the misbehavior forecaster and evaluate additional mutation and forecasting methods, such as the ones based on multi-horizon and multivariate time series.

REFERENCES

[1] Raja Ben Abdessalem, Annibale Panichella, Shiva Nejati, Lionel C. Briand, and Thomas Stifter. 2018. Testing Autonomous Cars for Feature Interaction Failures Using Many-objective Search. In *Proceedings of the 33rd ACM/IEEE International Conference on Automated Software Engineering (ASE 2018)*. ACM.

[2] Baidu. 2021. Apollo ADS platform. https://github.com/ApolloAuto/apollo

[3] BeamNG GmbH. 2018. BeamNG.research. https://beamng.gmbh/research/. Online; accessed 18 August 2019.

[4] R. Ben Abdessalem, S. Nejati, L. C. Briand, and T. Stifter. 2016. Testing advanced driver assistance systems using multi-objective search and neural networks. In *2016 31st IEEE/ACM International Conference on Automated Software Engineering (ASE)*.

[5] R. Ben Abdessalem, S. Nejati, L. C. Briand, and T. Stifter. 2018. Testing Vision-Based Control Systems Using Learnable Evolutionary Algorithms. In *2018 IEEE/ACM 40th International Conference on Software Engineering (ICSE)*.

[6] Matteo Biagiola, Andrea Stocco, Vincenzo Riccio, and Paolo Tonella. 2023. Two is Better Than One: Digital Siblings to Improve Autonomous Driving Testing. (2023). arXiv:2305.08060 [cs.SE]

[7] Mariusz Bojarski, Davide Del Testa, Daniel Dworakowski, Bernhard Firner, Beat Flepp, Prasoon Goyal, Lawrence D. Jackel, Mathew Monfort, Urs Muller, Jiakai Zhang, Xin Zhang, Jake Zhao, and Karol Zieba. 2016. End to End Learning for Self-Driving Cars. *CoRR* abs/1604.07316 (2016).

[8] Ardashir Bulsara, Adhiti Raman, Srivatsav Kamarajugadda, Matthias Schmid, and Venkat N Krovi. 2020. *Obstacle Avoidance Using Model Predictive Control: An Implementation and Validation Study Using Scaled Vehicles.* Technical Report. SAE Technical Paper.

[9] Georg Burkhard, S. Vos, N. Munzinger, E. Enders, and D. Schramm. 2018. Requirements on driving dynamics in autonomous driving with regard to motion and comfort. In *18. Internationales Stuttgarter Symposium*. Springer Fachmedien Wiesbaden.

[10] Li Chen, Penghao Wu, Kashyap Chitta, Bernhard Jaeger, Andreas Geiger, and Hongyang Li. 2023. End-to-end Autonomous Driving: Challenges and Frontiers. arXiv:2306.16927 [cs.RO]

[11] Mingfei Cheng, Yuan Zhou, and Xiaofei Xie. 2023. BehAVExplor: Behavior Diversity Guided Testing for Autonomous Driving Systems. In *Proceedings of the 32nd ACM SIGSOFT International Symposium on Software Testing and Analysis* (Seattle, WA, USA) *(ISSTA 2023)*. Association for Computing Machinery, New York, NY, USA, 488–500. https://doi.org/10.1145/3597926.3598072

[12] Kashyap Chitta, Aditya Prakash, Bernhard Jaeger, Zehao Yu, Katrin Renz, and Andreas Geiger. 2022. TransFuser: Imitation with Transformer-Based Sensor Fusion for Autonomous Driving. *Pattern Analysis and Machine Intelligence (PAMI)* (2022).

[13] Kyunghyun Cho, Bart Van Merriënboer, Caglar Gulcehre, Dzmitry Bahdanau, Fethi Bougares, Holger Schwenk, and Yoshua Bengio. 2014. Learning phrase representations using RNN encoder-decoder for statistical machine translation. *arXiv preprint arXiv:1406.1078* (2014).

[14] Jacob Cohen. 1988. *Statistical power analysis for the behavioral sciences*. L. Erlbaum Associates, Hillsdale, N.J.

[15] Department of Motor Vehicles, State of California. 2020. Autonomous Vehicle Collision Reports. https://www.dmv.ca.gov/portal/vehicle-industry-services/autonomous-vehicles/autonomous-vehicle-collision-reports/

[16] Alexey Dosovitskiy, Germán Ros, Felipe Codevilla, Antonio López, and Vladlen Koltun. 2017. CARLA: An Open Urban Driving Simulator. *CoRR* abs/1711.03938 (2017).

[17] EpicGames. 2023. UnrealEngine4. https://www.unrealengine.com.

[18] Hazem M. Fahmy, Mojtaba Bagherzadeh, Fabrizio Pastore, and Lionel C. Briand. 2020. Supporting DNN Safety Analysis and Retraining through Heatmap-based Unsupervised Learning. *CoRR* abs/2002.00863 (2020). arXiv:2002.00863 https://arxiv.org/abs/2002.00863

[19] Alessio Gambi, Marc Mueller, and Gordon Fraser. 2019. Automatically Testing Self-driving Cars with Search-based Procedural Content Generation. In *Proceedings of the 28th ACM SIGSOFT International Symposium on Software Testing and Analysis (ISSTA 2019)*. ACM.

[20] ESI Group. 2021. ESI PROSIVIC. https://myesi.esi-group.com/downloads/software-downloads/pro-sivic-2021.0.

[21] Fitash Ul Haq, Donghwan Shin, Shiva Nejati, and Lionel Briand. 2020. Comparing Offline and Online Testing of Deep Neural Networks: An Autonomous Car Case Study. In *Proceedings of 13th IEEE International Conference on Software Testing, Verification and Validation (ICST '20)*. IEEE.

[22] Fitash Ul Haq, Donghwan Shin, Shiva Nejati, and Lionel Briand. 2021. Can Offline Testing of Deep Neural Networks Replace Their Online Testing? A Case Study of Automated Driving Systems. *Empirical Softw. Engg.* 26, 5 (jul 2021), 30 pages. https://doi.org/10.1007/s10664-021-09982-4

[23] Kaiming He, Xiangyu Zhang, Shaoqing Ren, and Jian Sun. 2016. Deep Residual Learning for Image Recognition. In *2016 IEEE Conference on Computer Vision and Pattern Recognition (CVPR)*. 770–778. https://doi.org/10.1109/CVPR.2016.90

[24] Manzoor Hussain, Nazakat Ali, and Jang-Eui Hong. 2022. DeepGuard: A Framework for Safeguarding Autonomous Driving Systems from Inconsistent Behaviour. *Automated Software Engg.* 29, 1 (may 2022), 32 pages. https://doi.org/10.1007/s10515-021-00310-0

[25] Bernhard Jaeger, Kashyap Chitta, and Andreas Geiger. 2023. Hidden Biases of End-to-End Driving Models. *arXiv preprint arXiv:2306.07957* (2023).

[26] Saurabh Jha, Subho Sankar Banerjee, Timothy Tsai, Siva Kumar Sastry Hari, Michael B. Sullivan, Zbigniew T. Kalbarczyk, Stephen W. Keckler, and Ravishankar Krishnan Iyer. 2019. ML-Based Fault Injection for Autonomous Vehicles: A Case for Bayesian Fault Injection. *2019 49th Annual IEEE/IFIP International Conference on Dependable Systems and Networks (DSN)* (2019), 112–124. https://api.semanticscholar.org/CorpusID:195776612

[27] Xiaosong Jia, Yulu Gao, Li Chen, Junchi Yan, Patrick Langechuan Liu, and Hongyang Li. 2023. Driveadapter: Breaking the coupling barrier of perception and planning in end-to-end autonomous driving. In *Proceedings of the IEEE/CVF International Conference on Computer Vision*. 7953–7963.

[28] Xiaosong Jia, Penghao Wu, Li Chen, Jiangwei Xie, Conghui He, Junchi Yan, and Hongyang Li. 2023. Think Twice before Driving: Towards Scalable Decoders for End-to-End Autonomous Driving. In *Proceedings of the IEEE/CVF Conference on Computer Vision and Pattern Recognition*. 21983–21994.

[29] Shinpei Kato, Shota Tokunaga, Yuya Maruyama, Seiya Maeda, Manato Hirabayashi, Yuki Kitsukawa, Abraham Monrroy, Tomohito Ando, Yusuke Fujii, and Takuya Azumi. 2018. Autoware on Board: Enabling Autonomous Vehicles with Embedded Systems. In *2018 ACM/IEEE 9th International Conference on Cyber-Physical Systems (ICCPS)*. 287–296. https://doi.org/10.1109/ICCPS.2018.00035

[30] Prabhjot Kaur, Samira Taghavi, Zhaofeng Tian, and Weisong Shi. 2021. A Survey on Simulators for Testing Self-Driving Cars. arXiv:2101.05337 [cs.RO]

[31] Jinhan Kim, Robert Feldt, and Shin Yoo. 2019. Guiding Deep Learning System Testing Using Surprise Adequacy. In *Proceedings of the 41st International Conference on Software Engineering (ICSE '19)*. IEEE Press.

[32] Seulbae Kim, Major Liu, Junghwan "John" Rhee, Yuseok Jeon, Yonghwi Kwon, and Chung Hwan Kim. 2022. DriveFuzz. In *Proceedings of the 2022 ACM SIGSAC Conference on Computer and Communications Security*. ACM. https://doi.org/10.1145/3548606.3560558

[33] Diederik P. Kingma and Jimmy Ba. 2014. Adam: A Method for Stochastic Optimization. *CoRR* abs/1412.6980 (2014). https://api.semanticscholar.org/CorpusID:6628106

[34] Guanpeng Li, Yiran Li, Saurabh Jha, Timothy Tsai, Michael Sullivan, Siva Kumar Sastry Hari, Zbigniew Kalbarczyk, and Ravishankar Iyer. 2020. AV-FUZZER: Finding Safety Violations in Autonomous Driving Systems. In *2020 IEEE 31st International Symposium on Software Reliability Engineering (ISSRE)*. 25–36. https://doi.org/10.1109/ISSRE5003.2020.00012

[35] Guannan Lou, Yao Deng, Xi Zheng, Mengshi Zhang, and Tianyi Zhang. 2021. Testing of Autonomous Driving Systems: Where Are We and Where Should We Go? https://doi.org/10.48550/ARXIV.2106.12233

[36] Chengjie Lu, Yize Shi, Huihui Zhang, Man Zhang, Tiexin Wang, Tao Yue, and Shaukat Ali. 2023. Learning Configurations of Operating Environment of Autonomous Vehicles to Maximize their Collisions. *IEEE Transactions on Software Engineering* 49, 1 (2023), 384–402. https://doi.org/10.1109/TSE.2022.3150788

[37] Rhiannon Michelmore, Marta Kwiatkowska, and Yarin Gal. 2018. Evaluating Uncertainty Quantification in End-to-End Autonomous Driving Control. *CoRR* abs/1811.06817 (2018). arXiv:1811.06817

[38] Rhiannon Michelmore, Matthew Wicker, Luca Laurenti, Luca Cardelli, Yarin Gal, and Marta Kwiatkowska. 2020. Uncertainty Quantification with Statistical Guarantees in End-to-End Autonomous Driving Control. In *2020 IEEE International Conference on Robotics and Automation, ICRA*. IEEE, 7344–7350. https://doi.org/10.1109/ICRA40945.2020.9196844

[39] Mahshid Helali Moghadam, Markus Borg, Mehrdad Saadatmand, Seyed Jalaleddin Mousavirad, Markus Bohlin, and Björn Lisper. 2022. Machine Learning Testing in an ADAS Case Study Using Simulation-Integrated Bio-Inspired Search-Based Testing. https://doi.org/10.48550/ARXIV.2203.12026

[40] Galen E. Mullins, Paul G. Stankiewicz, R. Chad Hawthorne, and Satyandra K. Gupta. 2018. Adaptive generation of challenging scenarios for testing and evaluation of autonomous vehicles. *Journal of Systems and Software* 137 (2018).

[41] U.S. Department of Transportation. 2017. Traffic Safety Facts: Research Notes. https://crashstats.nhtsa.dot.gov/Api/Public/ViewPublication/812456.

[42] Kexin Pei, Yinzhi Cao, Junfeng Yang, and Suman Jana. 2017. DeepXplore: Automated Whitebox Testing of Deep Learning Systems. In *Proceedings of the 26th Symposium on Operating Systems Principles (SOSP '17)*. ACM.

[43] pylot. [n.d.]. Modular autonomous driving platform. https://pylot.readthedocs.io/en/latest/index.html. Online; accessed 11 Jenuary 2022.

[44] Vincenzo Riccio and Paolo Tonella. 2020. Model-Based Exploration of the Frontier of Behaviours for Deep Learning System Testing. In *Proceedings of ACM Joint European Software Engineering Conference and Symposium on the Foundations of Software Engineering (ESEC/FSE '20)*.

[45] Guodong Rong, Byung Hyun Shin, Hadi Tabatabaee, Qiang Lu, Steve Lemke, Mārtiņš Možeiko, Eric Boise, Geehoon Uhm, Mark Gerow, Shalin Mehta, et al. 2020. LGSVL Simulator: A High Fidelity Simulator for Autonomous Driving. *arXiv preprint arXiv:2005.03778* (2020).

[46] Hao Shao, Letian Wang, Ruobing Chen, Hongsheng Li, and Yu Liu. 2023. Safety-enhanced autonomous driving using interpretable sensor fusion transformer. In *Conference on Robot Learning*. PMLR, 726–737.

[47] Karen Simonyan and Andrew Zisserman. [n.d.]. Very Deep Convolutional Networks for Large-Scale Image Recognition. ([n. d.]). arXiv:1409.1556v6 [cs.CV]

[48] Siemens Digital Industries Software. 2023. Simcenter Prescan. https://www.plm.automation.siemens.com/global/en/products/simcenter/prescan.html.

[49] Andrea Stocco, Paulo J. Nunes, Marcelo d'Amorim, and Paolo Tonella. 2022. ThirdEye: Attention Maps for Safe Autonomous Driving Systems. In *Proceedings of 37th IEEE/ACM International Conference on Automated Software Engineering (ASE '22)*. IEEE/ACM. https://doi.org/10.1145/3551349.3556968

[50] Andrea Stocco, Brian Pulfer, and Paolo Tonella. 2022. Mind the Gap! A Study on the Transferability of Virtual vs Physical-world Testing of Autonomous Driving Systems. *IEEE Transactions on Software Engineering* (2022). https://doi.org/10.1109/TSE.2022.3202311

[51] Andrea Stocco and Paolo Tonella. 2021. Confidence-driven Weighted Retraining for Predicting Safety-Critical Failures in Autonomous Driving Systems. *Journal of Software: Evolution and Process* (2021). https://doi.org/10.1002/smr.2386

[52] Andrea Stocco, Michael Weiss, Marco Calzana, and Paolo Tonella. 2020. Misbehaviour Prediction for Autonomous Driving Systems. In *Proceedings of 42nd International Conference on Software Engineering (ICSE '20)*. ACM.

[53] Shuncheng Tang, Zhenya Zhang, Yi Zhang, Jixiang Zhou, Yan Guo, Shuang Liu, Shengjian Guo, Yan-Fu Li, Lei Ma, Yinxing Xue, and Yang Liu. 2022. A Survey on Automated Driving System Testing: Landscapes and Trends.

https://doi.org/10.48550/ARXIV.2206.05961
[54] CARLA team. 2023. CARLA: Leaderboard. https://leaderboard.carla.org/leaderboard/
[55] CARLA team. 2023. CARLA: Traffic Scenarios. https://leaderboard.carla.org/scenarios/
[56] Yuchi Tian, Kexin Pei, Suman Jana, and Baishakhi Ray. 2018. DeepTest: Automated Testing of Deep-neural-network-driven Autonomous Cars. In *Proceedings of the 40th International Conference on Software Engineering (ICSE '18)*. ACM.
[57] Foresee 2023. Replication Package. https://www.dropbox.com/scl/fo/5kr45r3f6l0ojih6k7j67/h?dl=0&rlkey=xn0dg28r94jgxss4lrhwcugq2.
[58] Udacity. 2017. A self-driving car simulator built with Unity. https://github.com/udacity/self-driving-car-sim. Online; accessed 18 August 2019.
[59] Fitash Ul Haq, Donghwan Shin, and Lionel C. Briand. 2023. Many-Objective Reinforcement Learning for Online Testing of DNN-Enabled Systems. In *2023 IEEE/ACM 45th International Conference on Software Engineering (ICSE)*. 1814–1826. https://doi.org/10.1109/ICSE48619.2023.00155
[60] Ashish Vaswani, Noam Shazeer, Niki Parmar, Jakob Uszkoreit, Llion Jones, Aidan N Gomez, Ł ukasz Kaiser, and Illia Polosukhin. 2017. Attention is All you Need. In *Advances in Neural Information Processing Systems*, I. Guyon, U. Von Luxburg, S. Bengio, H. Wallach, R. Fergus, S. Vishwanathan, and R. Garnett (Eds.), Vol. 30. Curran Associates, Inc. https://proceedings.neurips.cc/paper_files/paper/2017/file/3f5ee243547dee91fbd053c1c4a845aa-Paper.pdf
[61] Ankit Verma, Siddhesh Bagkar, Naga Venkata SaiTeja Allam, Adhiti Raman, Matthias Schmid, and Venkat N Krovi. 2021. Implementation and Validation of Behavior Cloning Using Scaled Vehicles. In *SAE WCX Digital Summit*. SAE International. https://doi.org/10.4271/2021-01-0248
[62] VISSIM. 2023. VISSIM website. https://www.ptvgroup.com/en-us/products/ptv-vissim.
[63] Frank Wilcoxon. 1945. Individual Comparisons by Ranking Methods. *Biometrics Bulletin* 1, 6 (Dec. 1945), 80. https://doi.org/10.2307/3001968
[64] Ekim Yurtsever, Jacob Lambert, Alexander Carballo, and Kazuya Takeda. 2020. A survey of autonomous driving: Common practices and emerging technologies. *IEEE access* 8 (2020), 58443–58469.
[65] Mengshi Zhang, Yuqun Zhang, Lingming Zhang, Cong Liu, and Sarfraz Khurshid. 2018. DeepRoad: GAN-based Metamorphic Testing and Input Validation Framework for Autonomous Driving Systems. In *Proceedings of the 33rd ACM/IEEE International Conference on Automated Software Engineering (ASE 2018)*. ACM.
[66] Ziyuan Zhong, Gail Kaiser, and Baishakhi Ray. 2021. Neural Network Guided Evolutionary Fuzzing for Finding Traffic Violations of Autonomous Vehicles.
[67] Tahereh Zohdinasab, Vincenzo Riccio, Alessio Gambi, and Paolo Tonella. 2021. DeepHyperion: Exploring the Feature Space of Deep Learning-Based Systems through Illumination Search. In *Proceedings of the ACM SIGSOFT International Symposium on Software Testing and Analysis (ISSTA '21)*. Association for Computing Machinery.